Microscopic origin of dimerization in the CuO_2 chains in $Sr_{14}Cu_{24}O_{41}$

Z. Hiroi
University of Antwerp (RUCA), Groenenborgerlaan 171, B-2020 Antwerpen, Belgium
and Institute for Chemical Research, Kyoto University, Uji, Kyoto 611, Japan

S. Amelinckx and G. Van Tendeloo
University of Antwerp (RUCA), Groenenborgerlaan 171, B-2020 Antwerpen, Belgium

N. Kobayashi
Institute for Chemical Research, Kyoto University, Uji, Kyoto 611, Japan

(Received 2 August 1996)

The interplay between structure and magnetic properties of $Sr_{14}Cu_{24}O_{41+\delta}$ with CuO_2 chain and Cu_2O_3 ladder building blocks is studied as a function of oxygen nonstoichiometry. The characteristic decrease in the magnetic susceptibility below 80 K for $\delta \approx 0$ disappears both with increasing and decreasing δ, and, correspondingly, the periodicity of the superstructure, which arises from the lattice mismatch along the chain direction between the two structure blocks, shows a significant change. The microscopic origin of the singlet ground state is suggested to be the localization of electrons at low temperature in dimers on structurally modulated CuO_2 chains. [S0163-1829(96)04946-6]

I. INTRODUCTION

The study of low-dimensional quantum magnets is one of the most important topics of contemporary solid-state physics. Recent progress in the study of superconductivity realized in the doped CuO_2 planes has strikingly demonstrated the rich physics associated with the $S=1/2$ Heisenberg antiferromagnetic square lattice. It stimulated work aiming at finding unknown intriguing phenomena principally governed by quantum effects in other classes of low-dimensional systems. The one most extensively studied recently is the spin ladder, which is a one-dimensional (1D) system comprising two parallel arrays of $S=1/2$ Heisenberg antiferromagnetic chains coupled antiferromagnetically.[1] Because of purely short-range spin correlation, a spin-liquid ground state with an energy gap has been predicted for even-leg spin ladders, and is now well established experimentally in the two-leg ladder compounds $(VO)_2P_2O_7$ and $SrCu_2O_3$.[2,3]

$A_{14}Cu_{24}O_{41}$ (A=Ca,Sr,Ba,La,Y) has attracted the interest of many experimentalists, because it also contains Cu_2O_3 ladder planes like those seen in $SrCu_2O_3$, as well as CuO_2 chains as seen in $CuGeO_3$ (Fig. 1).[4–7] Various magnetic measurements have shown that the compound exhibits a nonmagnetic ground state with an energy gap of 120–130 K.[8–13] A recent inelastic neutron-scattering study clearly revealed the existence of two kinds of energy gaps; the larger one of 400 K was attributed to the singlet-triplet excitation in the Cu_2O_3 ladder planes and the smaller one of 120 K to that in the CuO_2 chains.[13] The former is consistent with the theory and with previous experimental results on $SrCu_2O_3$, while the microscopic origin of the latter is still a question under discussion, partly because of the lack of detailed structural information.

One of the unique features of the compound under discussion, compared with $SrCu_2O_3$ and $CuGeO_3$, is that it already contains a certain number of holes in its stoichiometric composition. It has been pointed out in the case of the pure Sr compound that most holes present are located in the CuO_2 chains.[14] This suggests that we formally write the formula as $7(Sr_2Cu^{2+}{}_2O_3)$ (ladder)-$10(Cu^{2.6+}O_2)$ (chain), meaning that four Cu^{2+} spins per formula unit (f.u.) occur in the chains. Because one expects two spins per five copper atoms of the chains, it is plausible for singlet dimers to align periodically with a five-times interatomic spacing at low temperature, resulting in a nonmagnetic state. In contrast, a partial replacement of Sr by Ca gives rise to the transfer of holes from the chains to the ladder planes. Very recently, superconductivity at 12 K was reported under a high pressure of 3.5 GPa in the almost pure Ca compound, and suggested to occur in the doped spin-ladder planes.[15]

$Sr_{14}Cu_{24}O_{41}$ belongs to the class of so-called adaptive misfit compounds such as $MnSi_{2-x}$,[16] $Ba_{1-x}Fe_2S_4$,[17] and the MTS_3 family (M=Sn,Pb,Bi,...; S=Nb,Ta).[18] These compounds are generally based on two sublattices which are incompatible along one crystallographic direction, resulting in essentially 1D incommensurate structures. In most cases this incommensurability makes a precise structure determination difficult. According to the structural analysis on $Sr_{14}Cu_{24}O_{41}$ by McCarron *et al.*,[4] the ladder sublattice is face-centered-orthorhombic (space group $Fmmm$) with lattice parameters $a=11.459$ Å, $b=13.368$ Å, and $c_L=3.931$ Å. On the other hand the chain sublattice is A-centered orthorhombic (space group $Amma$) with nearly identical a and b parameters and a quite different c parameter of $c_C=2.749$ Å. Thus, a large misfit occurs along the c axis (along the chain or the ladder). These two sublattices are nearly commensurate at $7\times c_L=27.372$ Å and $10\times c_C=27.534$ Å. Strictly speaking, the title formulation is true only for $7\times c_L=10\times c_C$ ($c_L/c_C=10/7$). Even if one assumes the structure to be commensurate, a complete determination of the structure seems to be difficult in practice, because the crystal exhibits nonstoichiometry in oxygen as

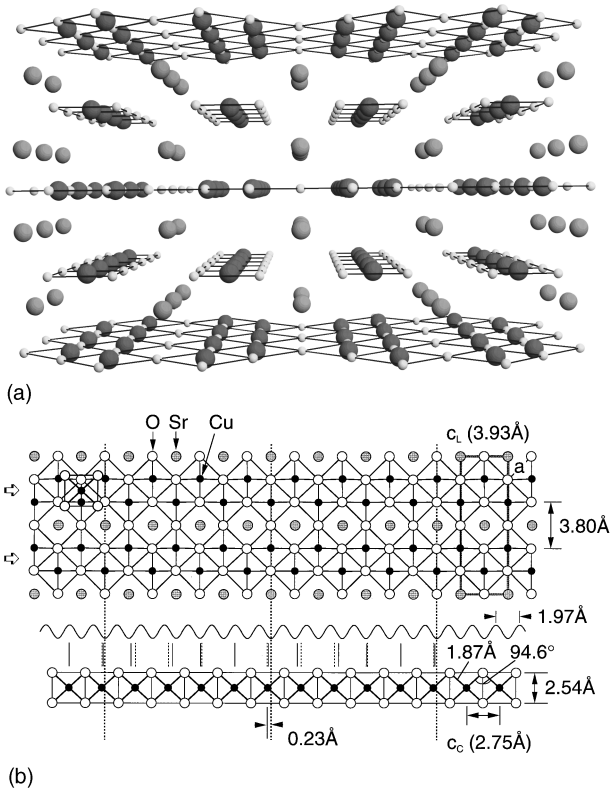

FIG. 1. (a) Perspective view of the crystal structure of $Sr_{14}Cu_{24}O_{41}$ along the chain/ladder direction. Large dark and bright spheres represent Cu and Sr atoms, respectively, and small ones oxygen atoms. (b) Schematic representation of two building blocks, a Cu_2O_3 two-leg ladder plane and a CuO_2 chain, in ideal $Sr_{14}Cu_{24}O_{41}$. The positions of atoms projected along the *b* axis are correctly shown on the basis of the structural refinement by McCarron *et al.* (Ref. 4). A CuO_2 chain sits above the middle of a Cu zigzag chain in a ladder plane (marked with arrows), and another Cu_2O_3 plane shifted by $c_L/2$ along the *c* axis with respect to the first one is put so as to sandwich the CuO_2 chain. The misfit between the *c*-axis lengths of the two blocks results in a 1D superstructure with a period of $7c_L=10c_C$. The sinusoidal wave drawn in between the ladder and the chain represents the misfit potential of a period of $c_L/2$. Vertical solid and dotted bars below that show the positions of Cu atoms of the chain with and without modifications by the misfit potential, respectively. See text for details.

well as in strontium content as reported in previous studies.[4] We believe that in the present compound the magnetic ground state and the structure must be strongly correlated, because the lattice misfit along the chain direction may induce a structural modulation in the chain, and, more important, the spacing of dimerized electrons expected in the ideal charge order state would coincide with the superlattice period due to the misfit.

In the present study we have investigated the structure of $Sr_{14}Cu_{24}O_{41+\delta}$ by means of electron diffraction (ED), as well as measured the static magnetic susceptibility. It has been found that oxygen nonstoichiometry occurs over a wide range of δ values $-0.7\leqslant\delta\leqslant 0.9$, and both the magnetic properties and the superstructure change with δ. The structural characterization based on a modified version of the ''cut and projection'' method[19] suggests that, in the presence of a certain periodic electrostatic potential imposed by the ''rigid'' ladder block (we call it the misfit potential), the uniform more deformable chain can be transformed into various 1D sequences of Cu dimers and trimers, depending on the magnitude of the misfit. Associating spin singlets with the dimers gives a reasonable explanation for the observed experimental results.

II. EXPERIMENT

A pellet of $Sr_{14}Cu_{24}O_{41}$ was prepared by the standard solid-state reaction method. An appropriate mixture of $SrCO_3$ and CuO was heated at 1000 °C in air for several times with intermittent grindings, followed by quenching. A series of polycrystalline samples with different oxygen content was prepared by annealing a portion of the pellet at different temperatures in air or in an oxygen or an argon flow for 24 h. Samples with higher oxygen content were prepared by annealing under high oxygen pressures (6 GPa) using $KClO_4$ as an oxygen generator in a high-pressure apparatus.[20] The oxygen content was determined within the experimental precision of ± 0.1 by heating to 800 °C in a 95% N_2-5% H_2 and measuring the weight loss. Annealing under extremely reducing and oxidizing conditions resulted in decomposition of the material. Nearly single-phase samples were obtained for oxygen content between $O_{40.3}$ and $O_{41.9}$.

Magnetic susceptibility was measured in a superconducting quantum interference device magnetometer in an applied magnetic field of 1 T on heating after rapid cooling to 5 K in a nearly zero field. ED experiments were performed in a 200 kV electron microscope (CM-20) at room temperature and also in a 300 kV electron microscope (CM-30) at ~14 K for selected samples.

III. RESULTS

A. Magnetic susceptibility

The temperature dependence of the magnetic susceptibility χ has been found to be strongly dependent on oxygen nonstoichiometry as shown in Fig. 2. The near-stoichiometric sample ($\delta=0.0$) shows a characteristic decrease in χ below 80 K, followed by an upturn below 20 K due to a Curie contribution. The curve is almost identical to those reported previously.[8,9] However, in both reduced and oxidized samples, this gaplike behavior becomes less clear, and instead the Curie component increases with increasing deviation from the ideal oxygen content O_{41}. Such tendency is more pronounced in the oxidized samples. Susceptibility measurements mostly reveal the contribution from Cu^{2+} spins on the chains, because the Cu_2O_3 plane with a large spin gap of 400 K should be almost magnetically inactive in this temperature range. Following the previous approach,[10] we assume singlet dimer formation on the chains. Then, χ should be described as a sum of a temperature-independent term χ_0, a Curie-Weiss term χ_C, and a dimer term χ_D in units of emu/mol Cu;

$$\chi=\chi_0+\chi_C+\chi_D. \tag{1}$$

χ_C and χ_D are described as

$$\chi_C=C/(T-\Theta), \quad C=N_F(N_A/24)g^2\mu_B^2/4k_B, \tag{2}$$

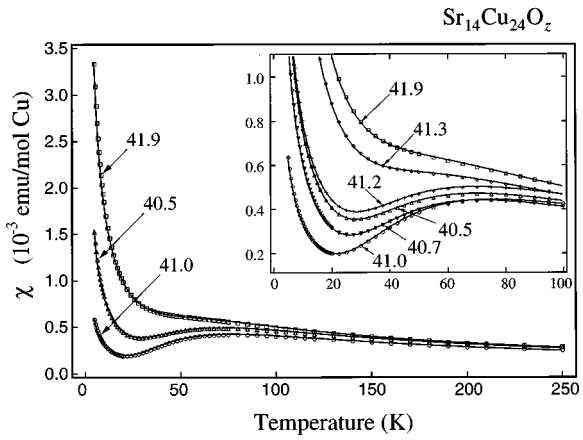

(a)

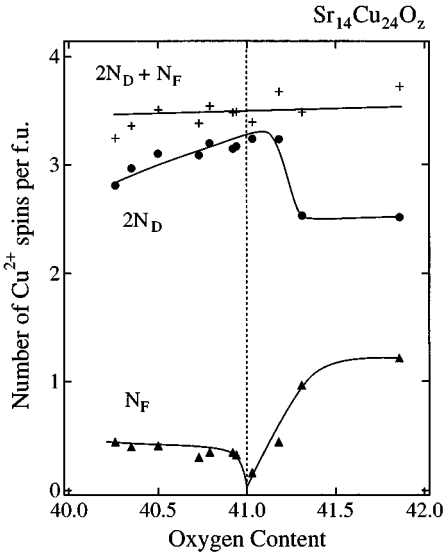

(b)

FIG. 2. (a) Temperature dependence of static magnetic susceptibility χ for a series of polycrystalline samples with various oxygen content. For clarity only data sets of representative samples are shown. In each data set marks represent data points, and a solid line is a fit to Eq. (1) as described in text. (b) Variations of the density of dimerized spins $2N_D$ and free spins N_F as well as their sum as a function of oxygen content. Solid lines are guides to the eye.

$$\chi_D = 2N_D(N_A/24)g^2\mu_B^2/\{k_BT[3+\exp(J_D/k_BT)]\}, \quad (3)$$

with N_F free $S=1/2$ spins per f.u., N_D dimers per f.u., and a dimer coupling constant J_D. N_A and k_B are the Avogadro number and the Boltzmann constant, respectively. The g factor is set to 2.2 from the literature.[9] The results of fitting are very good for all the data sets as shown in Fig. 2. For $\delta=0.0$ we find that there are $N_D=1.62(1)$ dimers per f.u. [or 3.24(2) spins per f.u.] with $J_D=130.9(4)$ K, a free spin density $N_F=0.157(1)$ spins per f.u. and $\Theta=0.23(3)$ K, and $\chi_0=4.4(2)\times10^{-5}$ emu/mol Cu. J_D, χ_0, and Θ are only weakly dependent on oxygen content, while $2N_D$ and N_F vary significantly as shown in Fig. 2(b). $2N_D$ shows a broad peak at $\delta=0$, while N_F rapidly decreases to zero at $\delta=0$. Note that the δ dependence of both $2N_D$ and N_F is much stronger for $\delta>0$ than for $\delta<0$, which will be discussed below in terms of the structure. The total spin density $2N_D+N_F$ is about 3.5, which is smaller than expected from the ideal composition. This may be related to nonstoichiometry in metal composition, as was pointed out in previous work:[4] Assuming only 2% of Sr vacancies per f.u. for $\delta=0$ could explain this reduction in the total spin density. Moreover, the total spin density is almost independent of δ. This is unusual from the viewpoint of charge neutrality, because, for example, a change of 0.5 in oxygen content per f.u. should change the spin density by 1 per f.u. The reason is not clear but may also be related to nonstoichiometry in metal composition. Probably corresponding to this, resistivity did not change so much with oxygen content; its magnitude slightly decreased with increasing oxygen content, and the temperature dependence always showed an insulating behavior.

B. Electron diffraction

Electron-diffraction patterns in misfit compounds are generally complicated because of multiple diffraction and incommensurability. In the present crystal the most dense section of the reciprocal lattice is seen in the $[1\bar{1}0]$ zone axis. As shown in Fig. 3, the $[1\bar{1}0]$ ED pattern consists of two centered rectangular meshes of intense spots as well as of weak spots which form complex rows along the c^* axis. This is similar to those reported for $(Ca,Sr)_{14}Cu_{24}O_{41}$.[21,22] The smaller mesh corresponds to the ladder sublattice and the larger one to the chain sublattice.

The satellite sequences can be interpreted as being generated by multiple diffraction. It is also possible to associate them with the structural modulation of the two interpenetrating structures. However, to distinguish one from the other experimentally is almost impossible. Here we measured on the negatives the ratio of the c parameters of the two sublattices, $\alpha=c_L/c_C$, in order to estimate the magnitude of the misfit. Because the origin of the superstructure is apparently the misfit, the superlattice period Λ is uniquely related to α. Assuming that mc_L and nc_C spacings (m,n=integers) are included in Λ, $\alpha=c_L/c_C=n/m$. For the stoichiometric composition $\alpha=10/7\approx1.428$.

A series of samples with $\delta=-0.7$, -0.2, 0.0, and 0.9 have been investigated by using ED. Representative ED patterns obtained from the samples with $\delta=0.0$ and -0.7 are shown in Figs. 3(a) and 3(b), respectively. The measured α values are 1.416 and 1.441, respectively. This small difference in α is visually detected as a difference in the spacings of certain satellite spots as shown in the inset to Fig. 3. Note that the overall features apart from the magnitude of the misfit are substantially the same for the two patterns. From each sample a number of fragments from 20 to 40 were examined in a microscope, and the histogram of Fig. 4 was obtained. It was necessary to proceed statistically, because even slight fluctuations in composition could result in inhomogeneity, which might be inevitable in such a delicate material. It is obviously recognized from Fig. 4 that α shows significant deviations from an ideal value of 10/7 for $\delta\neq0$. At the minimum oxygen content α is close to another commensurate approximation of 13/9, while a rather broad distribution around 10/7 appears at $\delta=0.0$. A near-stoichiometric powder sample prepared by Kato was also examined by electron mi-

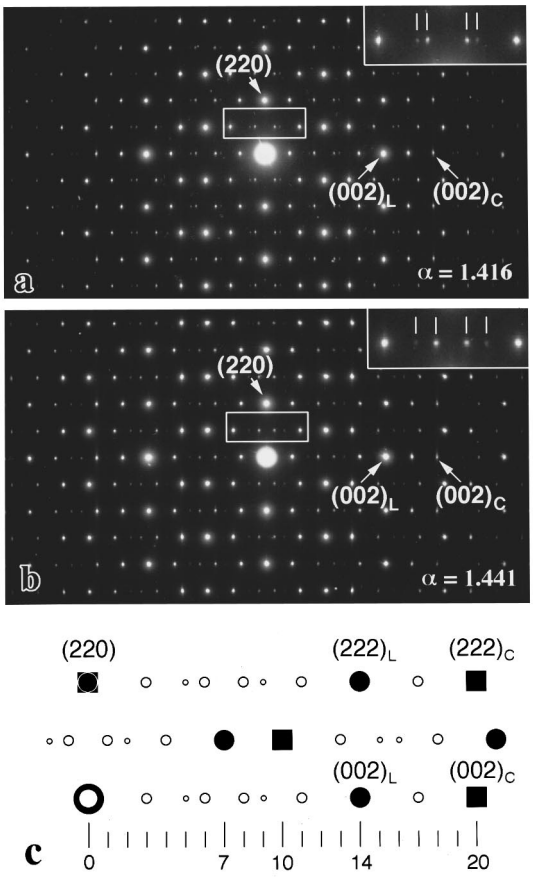

FIG. 3. [$1\bar{1}0$] zone axis ED patterns obtained from the samples with $\delta=0.0$ (a) and -0.7 (b), and schematic representation for $\alpha=10/7$ (c). A rectangle containing satellite spots near the (110) reflection is enlarged and shown to the inset. A slight difference in α between the two patterns is well detectable in the comparison of the spacings of these satellite spots. In the schematic representation in (c), filled circles and squares show the positions of fundamental reflections coming from the ladder and the chain sublattices, respectively, and small open circles show those of satellite reflections.

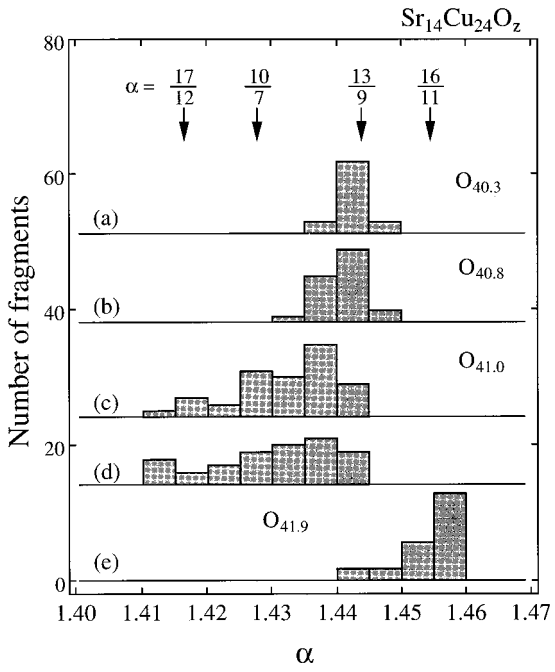

FIG. 4. Histograms showing the distribution in α determined by using ED for samples with $\delta=-0.7$ (a), -0.2 (b), 0.0 (c), 0.9 (e), and the sample prepared by Kato (d). The vertical axis shows the number of fragments examined in an electron microscope. Positions of typical commensurate descriptions of α are shown with arrows at the top of the figure.

croscopy and found to show a broad distribution around 10/7 similar as observed in the $\delta=0.0$ sample. Further, the increase of δ gives again a more rapid increase and a sharp distribution in α. The accuracy of determining α from ED experiments is not obvious. However, judging from the sharp distribution observed for the off-stoichiometric samples, it must be within 0.005, enough for the present analysis. Then, the broad distribution for $\delta\approx 0$ implies that even a small change in local oxygen content results in a considerable change in the misfit especially near the stoichiometric composition. This suggests an experimental difficulty in obtaining a homogeneous, stoichiometric sample; it may also diminish the free magnetic moments as will be discussed later.

The misfit must be related not only to the density of holes but also to oxygen defects. It is expected from the former contribution, assuming all holes in the chains, that the misfit decreases monotonously with increasing δ, because the average interatomic distance in the chains should decrease with increasing hole density ($\alpha=c_L/c_C$). This is the case observed for $\delta<0$. However, the observed sudden increase in α for $\delta>0$ suggests that particularly excess oxygens, possibly in the Sr layers between the ladder and the chain layers, play also a substantial role in determining the misfit. Crystallographic data to show where oxygen vacancies or excess oxygens occur is necessary for further discussion. To be noted here is that the observed change in the misfit as a function of oxygen content is apparently closely correlated with the corresponding change in χ, especially with $2N_D$ and N_F, suggesting that the microscopic origin of dimerization is related to the superstructure.

We also checked samples with $\delta=0.0$ and 0.9 in an electron microscope at low temperature (~ 14 K), well below the magnetic transition temperature. However, no substantial change in periodicity was detected: No lock-in transitions to $\alpha=10/7$ were observed. In addition, we did not observe any detectable change in the relative intensity of the superlattice reflections. These mean that the magnetic transition takes place without the formation of additional superstructures or without a large change in the preexisting superstructure as detectable in ED.

IV. DISCUSSION

A. Structural description

We now consider more details of the superstructure. As depicted in Fig. 1, a CuO_2 chain sits exactly above the middle of a Cu zigzag chain in the ladder plane with a certain phase shift along the c axis.[4] A second zigzag chain shifted by $c_L/2$ along the c axis with respect to the first one sits above the CuO_2 chain. Thus, the CuO_2 chain experiences an electrostatic potential (misfit potential) with a period of $c_L/2$ caused by the relatively rigid ladder planes

above and below, as schematically shown by a sinusoidal wave in Fig. 1. It is quite reasonable to assume that the relatively ''soft'' CuO_2 chain will be deformed by that potential of which the period does not fit that of the chain.[5] This is found to be the case in other misfit compounds.[18] It is assumed that the minimum of the misfit potential occurs in phase with the Cu-O rows of the ladders running along the c axis, because locating the CuO_4 square of the chain on the ladder plane at the position as depicted in the top-left of the figure may be the most energetically favorable to minimize electrostatic repulsion between large oxygen ions in the chain and the ladder. The most probable deformation pattern is illustrated in the figure, where the dotted bars represent the unrelaxed positions of the Cu atoms in the chain and the solid bars the relaxed positions. Remarkably, there appear two neighboring Cu atoms with an increased distance, separated by three Cu atoms with rather shorter bond lengths. This means that the uniform chain would hypothetically be transformed into 1D sequences of dimers and trimers in the presence of the misfit potential. Because Cu^{2+} ions have larger ionic radii than Cu^{3+} ions, they must prefer expanded positions: They would form pairs at dimerized sites. Such charge ordering would be possible if the stabilization due to the deformation (or the constriction by the misfit) is sufficient to compensate for the Coulomb repulsion arising from the charge order.

It is interesting to compare the CuO_2 chains in the present compound with similar chains found in $CuGeO_3$.[23] In the isomorphous compound $(Ca_8La_6)Cu_{24}O_{41}$ with all copper ions in the divalent state a weakly ferromagnetic interaction between neighboring Cu^{2+} spins in the CuO_2 chain was found,[10] which was assigned to nearly 90° Cu-O-Cu superexchange bonds [about 93° for $(Ca_8La_6)Cu_{24}O_{41}$ and 94.6° for $Sr_{14}Cu_{24}O_{41}$ evaluated from their crystallographic data[4,5]]. In contrast, antiferromagnetic interactions of 100 K are known for the CuO_2 chains in $CuGeO_3$ with a larger bond angle of 98.7°. This implies that even a slight increase in the Cu-Cu distance and a change in the angle of the superexchange bonds could switch the magnetic interaction from ferromagnetic to antiferromagnetic. Therefore, a pair of spins trapped at the expanded dimer sites presumably form a singlet state due to antiferromagnetic interaction. To confirm this scenario, we need a detailed structural analysis of an ideal $Sr_{14}Cu_{24}O_{41}$ crystal, taking into account the modulations.

B. Structure model describing the charge order and dimerization

So far we have discussed only the ideal commensurate superstructure for $\alpha=10/7$. However, the key to understanding the relation between magnetism and superstructure is to be found in the nonideal cases, i.e., for $\alpha\neq 10/7$ $(\delta\neq 0)$. It is particularly important to know the origin of the free magnetic moments. We apply a modified version of the ''cut and projection'' method to derive the essentially incommensurate structures. The original method is well known in the field of quasicrystals[24] and it has been applied in its modified version to the interpretation of complex superstructures in some inorganic compounds.[19] It derives intuitively a 1D uniform sequence containing two different spacings, l and s, which best fits an actual commensurate or incommensurate superlattice period.

Consider a 2D orthogonal lattice constructed on base vectors with lengths of l and s [Fig. 5(a)]. Every 1D sequence of l and s spacings can uniquely be represented in the 2D space as a stepped line. Consider now a sequence composed of p l spacings and q s spacings. If the sequence is required to be uniform, spacings at any point must be as close as possible to the average value $d=(pl+qs)/(p+q)$. Hence, the stepped line has to be as close as possible, at any point, to a straight line E passing through the origin, with a slope given by

$$\tan\theta=qs/pl=[(l-d)/(d-s)](s/l). \tag{4}$$

It is easy to see that all the nodes of the stepped sequence derived in this way belong to a strip obtained by sliding one unit cell along E. The 1D sequence of $L=l/\sqrt{2}$ and $S=s/\sqrt{2}$ spacings can now be obtained by projecting the zigzag line within the strip (including either the top or the bottom line) onto a line P with a 45° slope. This particular angle ensures that the ratio of the lengths of the L and S units remains the same as that of l and s through the projection.[19]

In the present case, this average value of d should correspond to a near-coincidence distance between the two c-axis lengths, $1/d=1/c_2-1/c_1$, where $c_1=c_C\approx 2.7$ Å and $c_2=c_L/2\approx 1.95$ Å. Considering a sequence in the CuO_2 chain, d $(\approx 7$ Å) is larger than $2c_C$ and smaller than $3c_C$, which means that a sequence can be described with two basic lengths of $l=3c_C$ and $s=2c_C$. Then, the slope is given as

$$\begin{aligned}\tan\theta&=[(3c_C-d)/(d-2c_C)](2/3)\\&=[(6-4\alpha)/(3\alpha-4)](2/3).\end{aligned} \tag{5}$$

This equation shows that a change in α is reflected by a change in the slope which determines a possible 1D sequence composed of $2c_C$ (dimer) and $3c_C$ (trimer). For $\alpha=10/7$ the sequence is described as 232323 . . . [Fig. 5(b)], which must correspond to such a possible structural modulation occurring in the presence of the misfit potential as described before. Interestingly, when α is increased (the slope is decreased), this regular sequence is interrupted by a pair of trimers like $\underline{33}2323\underline{33}23\cdots$ for $\alpha=13/9$, where the two sublattices are commensurate at $13c_C$ and $9c_L$. The density of dimers decreases with increasing α as depicted in Fig. 5(b). On the other hand, the regular sequence is interrupted by a pair of dimers in the case of $\alpha<10/7$.

Then, the model can present a possible spin configuration in the CuO_2 chain, if one associates antiferromagnetically coupled spins with the dimers. In the ideal case of $\alpha=10/7$ and $2N_D=4$, perfect charge ordering is expected with such a well ordered arrangement of dimerized spins as illustrated in the figure. The most important implication from the model is that the decrease of dimer density with increasing α would produce excess unpaired spins on trimers which could be the origin of the free Cu^{2+} moments observed in the susceptibility measurements. Therefore, it is meaningful to count the number of spins on the model which can be compared with the experimental data. Let us assume that the total number of spins is always 3.5 per f.u. (0.35 per Cu on the chain). For

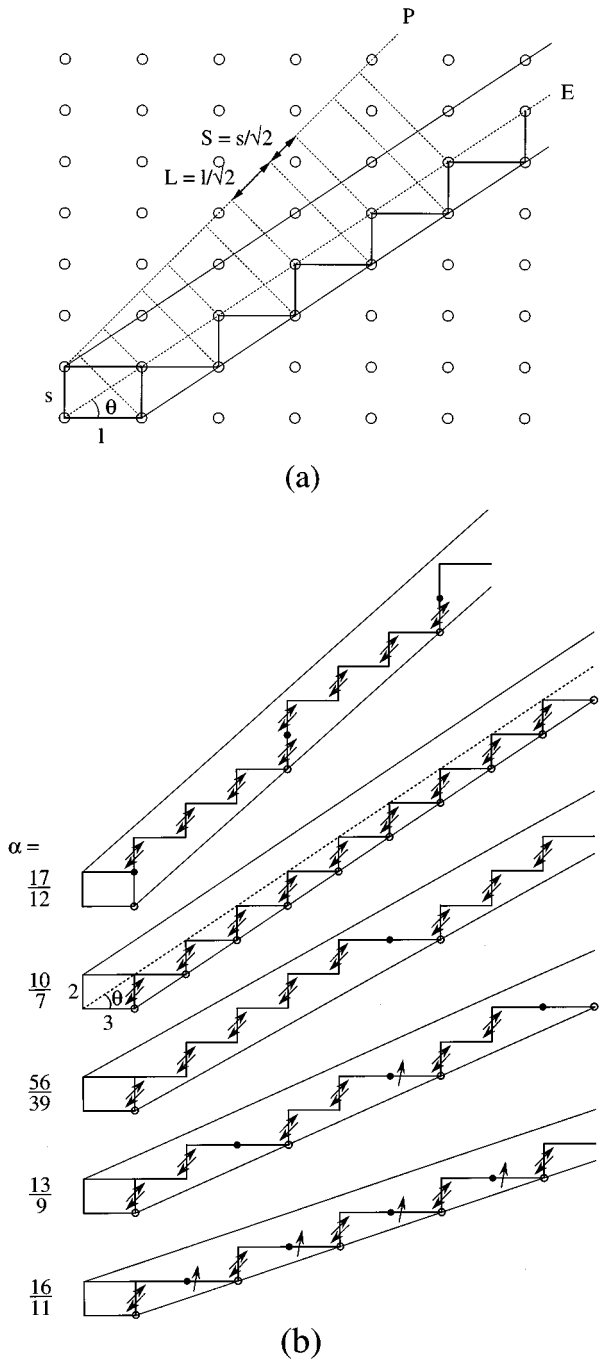

FIG. 5. (a) Modified version of the cut and projection method describing a uniform sequence of long (L) and short (S) segments ($\tan\theta = s/l$); $SLSLSL\ldots$ (Ref. 19). (b) Application of the method to the present superstructures; $s=2$, $l=3$, and $\tan\theta$ given in Eq. (5). Each stepped zigzag line presents a possible 1D sequence of $2c_C$ and $3c_C$ spacings in the CuO_2 chain for a selected α value. Derived commensurate 1D sequences are [2232323][$(\alpha,\tan\theta)$ $=(17/12,7/9)$], [23] (10/7,6/9), [23232323233] (56/39,5/9), [23233] (13/9,4/9), and [233] (16/11,3/9). A vertical line in the stepped lines corresponds to a Cu dimer, and a horizontal line a Cu trimer. Dimerized spins depicted with a pair of parallel arrows should be located on the Cu dimer. Excess uncoupled spins may occur on the trimer sites for $\alpha > 10/7$, giving rise to free moments as observed in magnetic-susceptibility measurements.

the ideal case of $\alpha = 10/7$ ($\delta = 0$) the density of dimerized Cu atoms is larger than that of spins, and, thus, N_F should be close to zero. The residual Curie component observed for the $\delta = 0.0$ sample must come from inhomogeneity of the sample which is actually seen as a broad distribution in α in Fig. 4. As α increases slightly, for example, for $\alpha = 13/9$, the model predicts that 4.55 spins per 13 Cu atoms (which is the number expected from the total number of spins of 3.5 per f.u.) should be divided into two coupled spins on dimers and 0.55 uncoupled spins on trimers. This division is reduced to $(2N_D, N_F) = (3.08, 0.42)$, which is close to the experimental values for $\delta < 0$. A gradual increase in $2N_D$ and a decrease in N_F to zero with increasing δ in Fig. 2(b) may reflect a gradual change in α from 13/9 to 10/7 as seen in Fig. 4. On the other hand, α seems to increase more rapidly in the case of $\delta > 0$. Considering the appropriate model for $\alpha = 16/11$, the number of surviving dimers is only one per eight Cu atoms (the total number of spins is 2.8 per eight Cu), which gives $(2N_D, N_F) = (2.5, 1.0)$, again in good agreement with the data for $\delta = 0.9$. In contrast, a decrease in α from 10/7, which is partly seen only for the $\delta = 0.0$ sample, may not cause an increase in the free spin density, because a pair of dimer sites appearing with decreasing α may produce enough sites for coupled spins. Therefore, we can quantitatively explain the observed magnetic susceptibility by assuming the distribution of spins in the chains derived from the present model.

Recently an inelastic neutron study on $(Ca_{0.2}Sr_{0.8})_{14}Cu_{24}O_{41}$ by Eccleston, Azuma, and Takano suggested that portions of the CuO_2 chains are dimerized or broken up into larger finite chains by nonmagnetic CuO_2 units.[13] This may correspond to the present model with $\alpha > 10/7$, and, thus, their sample was presumably nonstoichiometric in oxygen or metal content. It was previously reported that a large amount of oxygen loss occurred for such Ca-substituted samples.[11,14]

V. CONCLUSION

We have studied the charge order and dimerization in the CuO_2 chains in $Sr_{14}Cu_{24}O_{41}$ from a structural point of view. An intimate relation between magnetism and superstructures arising from the lattice misfit has been revealed as a function of oxygen nonstoichiometry. The number of dimerized and free spins estimated from the susceptibility measurements is consistent with the model based on the modification of the structure of the chains due to the misfit potential produced by the ladder layers.

It is not clear whether the lattice distortion actually exists at high temperature or appears with the change in electronic structure at low temperature. We observed no change in superlattice reflections in our ED experiments at low temperature. However, it would be impossible to detect in ED experiments such a lattice distortion as occurring if the periodicity is the same as that of the superlattice due to the lattice misfit. It is evident from the present study that the main features of the charge ordered state are determined by the misfit potential. Thus, we think that itinerant electrons in the CuO_2 chains at high temperature tend to be localized in dimers in a given misfit potential as temperature decreases below a dimer coupling energy J_D. It should be classified into a class of a singlet ground state different from the spin-

Peierls transition, because the misfit potential plays the important role instead of the phonons.

ACKNOWLEDGMENTS

The authors express their special thanks to H.-U. Nissen and R. Wessicken for their help in the ED experiments at low temperature, and also to M. Kato and M. Azuma for sending their samples for preliminary ED experiments. A fruitful discussion with T. M. Rice and M. Sigrist is acknowledged. Z.H. is grateful for the bilateral programs for scientist exchanges between Japan Society for the Promotion of Science and National Foundation for Scientific Research of Belgium.

[1] E. Dagotto and T. M. Rice, Science **271**, 618 (1996).
[2] R. S. Eccleston, T. Barnes, J. Brody, and J. W. Johnson, Phys. Rev. Lett. **73**, 2626 (1994).
[3] M. Azuma, Z. Hiroi, M. Takano, K. Ishida, and Y. Kitaoka, Phys. Rev. Lett. **73**, 3463 (1994).
[4] E. M. McCarron, M. A. Subramanian, J. C. Calabrese, and R. L. Harlow, Mater. Res. Bull. **23**, 1355 (1988).
[5] T. Siegrist, L. F. Schneemeyer, S. A. Sunshine, and J. V. Waszczak, Mater. Res. Bull. **23**, 1429 (1988).
[6] R. S. Roth, C. J. Rawn, J. J. Ritter, and B. P. Burton, J. Am. Ceram. Soc. **72**, 1545 (1989).
[7] M. W. McElfresh, J. M. Coey, P. Strobel, and S. V. Molnar, Phys. Rev. B **40**, 825 (1989).
[8] M. Kato, H. Chizawa, Y. Koike, T. Noji, and Y. Saito, Physica C **235-240**, 1327 (1994).
[9] M. Matsuda and K. Katsumata (unpublished).
[10] S. A. Carter, B. Batlogg, R. J. Cava, J. J. Krajewski, J. W. F. Peck, and T. M. Rice, Phys. Rev. Lett. **77**, 1378 (1996).
[11] M. Uehara, M. Ogawa, and J. Akimitsu, Physica C **255**, 193 (1995).
[12] M. Matsuda, K. Katsumata, H. Eisaki, N. Motoyama, S. Uchida, S. M. Shapiro, and G. Shirane, Phys. Rev. B (to be published).
[13] R. S. Eccleston, M. Azuma, and M. Takano, Phys. Rev. B **53**, 14 721 (1996).
[14] M. Kato, K. Shiota, and Y. Koike, Physica C **258**, 284 (1996).
[15] M. Uehara, T. Nagata, J. Akimitsu, H. Takahashi, N. Mori, and K. Kinoshita, J. Phys. Soc. Jpn. (to be published).
[16] H. Nowotny, in *The Chemistry of Extended Defects in Non-Metallic Solids*, edited by L. Eyring and M. O'Keefe (North-Holland, Amsterdam, 1970), p. 223.
[17] N. Nakayama, K. Kosuge, and S. Kachi, J. Solid Chem. **36**, 9 (1981).
[18] G. A. Wiegers, A. Meetsma, S. V. Smaalen, R. J. Haange, J. Wulff, T. Zeinstra, J. L. d. Boer, S. Kuypers, G. Van Tendeloo, J. Van Landuyt, S. Amelinckx, A. Meerschaut, P. Rabu, and J. Rouxel, Solid State Commun. **70**, 409 (1989).
[19] S. Amelinckx and D. Van Dyck, in *Electron Diffraction Techniques*, edited by J. M. Cowley (Oxford University Press, Oxford, 1993), Vol. 2, p. 309.
[20] Z. Hiroi, M. Azuma, M. Takano, and Y. Bando, Physica C **208**, 286 (1993).
[21] X. J. Wu, E. Takayama-Muromachi, S. Suehara, and S. Horiuchi, Acta Crystallogr. A **47**, 727 (1991).
[22] O. Milat, G. Van Tendeloo, S. Amelinckx, M. Mehbod, and R. Deltour, Acta Crystallogr. A **48**, 618 (1992).
[23] M. Hase, I. Terasaki, and K. Uchinokura, Phys. Rev. Lett. **70**, 3651 (1993).
[24] A. Katz and M. Duneau, Phys. Rev. Lett. **54**, 2688 (1985).